SEP. 2020- DEC. 2020 • Volume XXI Number III

THE ASEAN JOURNAL OF RADIOLOGY

Highlight

- Original Article
- Case Report
- Classic Case
- ASEAN Movement in Radiology

Official Journal of
The Royal College of Radiologists of Thailand,
ASEAN Association of Radiology, and
Foundation for Orphan and Rare Lung Disease

ISSN 2672-9393

The ASEAN
Journal of Radiology

CONTENTS

THE ASEAN JOURNAL OF RADIOLOGY
ISSN 2672-9393

From The Editor

Received 27 December 2020; accepted 27 December 2020
doi:10.46475/aseanjr.v21i3.102

The editor is visiting Professor Vimol Sukthomya, his respected teacher, in Chiangmai, the largest city in Northern Thailand.

The health of one nation in human web

The pandemic of COVID-19 seems to be going on with no sign of its ending.

In case of Thailand, long before this December, most of the newly infected individuals were mainly those who entered Thailand by air route. At that time, due to the lack of a policy for active searching for infected individuals within the border, together with a shortage of affordable testing kits and an effective tracking system, the asymptomatic domestic infection cannot be estimated.

In the mid of this month, there were reported Thai patients who used to work in Myanmar and illegally crossed the border to Thailand. Not so long after the aforementioned domestic outbreak, there were tremendously larger number of domestic infected cases among Myanmar workers in the central Thailand, who were also suspected to be illegal immigrants.

The recently reported number of domestic infected cases which was higher than the beginning of the outbreak was thought to be caused by the crowded living condition of foreign workers on one hand. On the other hand, the higher reported number may stem from the more active searching of asymptomatic infected individuals, which was made possible by more affordable testing kits and a more effective tracking technology.

Thailand shares her long west border with Myanmar from the most top to the upper southern part. With the much lower birth rate comparing to her neighbouring countries, Thailand requires the imported workforce, mainly from Myanmar.

In the beginning of the year due to the outbreak of COVID 19, the income of various business sectors has been greatly reduced; many were out of business, especially the service and tourism sectors. In order to cope with the situation, many employees were laid out. To save the cost of living while waiting for the better situation to get reemployed, those workers came back to their hometowns where they did not have to rent houses or pay for expensive food. However,

the situation of the COVID 19 epidemic was much worse in Myanmar who shares her west border with India. The COVID 19 epidemic in Myanmar leads to a great economic downfall in which the basic household income cannot be fulfilled by a great number of households. Thus, many were forced to seek work in Thailand as fast as they could and the only way out was illegal immigration to Thailand.

Besides, the vast area of the natural border between Thailand and Myanmar makes it extremely hard to prevent from illegal immigration; many criticized the ineffectiveness of border protection or even raised the question of the possibility of corruption among border officers who might be assisting in the illegal immigration.

At the end of the day, we have to admit that humans are social beings whose survivals are dependent upon each other which inevitably leads to an exchange of resources and continual migration. The containment of COVID-19 within a country is far from possible because we rely on interaction with one another, whether inside or across the border.

Wiwatana Tanomkiat, M.D.
Editor,
The ASEAN Journal of Radiology
Email: aseanjournalradiology@gmail.com

THE ASEAN JOURNAL OF RADIOLOGY
ISSN 2672-9393

Original Article

Abdominal CT radiation dose optimization at Siriraj Hospital (phase II)

Piyaporn Apisarnthanarak, M.D.
Suchanya Hongpinyo, M.D.
Krittya Saysivanon, B.Sc.
Chulaluck Boonma, B.Sc.
Sureerat Janpanich, RN.
Preeyanuch Ketkan, RN.
Kobkun Muangsomboon, M.D.
Wanwarang Teerasamit, M.D.
Sopa Pongpornsup, M.D.
Pairash Saiviroonporn, Ph.D.
From Department of Radiology, Faculty of Medicine Siriraj Hospital, Mahidol University, Bangkok, Thailand.
Address correspondence to P.A. (e-mail: punpae159@gmail.com)

Received 28 April 2020; revised 12 December 2020; accepted 14 December 2020
doi:10.46475/aseanjr.v21i3.81

Abstract

Objective: To compare radiation dose, radiologists' satisfaction, and image noise between the standard dose abdominal CT currently performed at our hospital and the new automatic tube current modulation (ATCM) low dose abdominal CT, using various parameters (0%, 10%, 20%, and 30%) of the Adaptive Statistical Iterative Reconstruction (ASiR).

Materials and Methods: We prospectively performed the ATCM low dose abdominal CT in 111 participants who had prior standard dose CT for comparison. The ATCM low dose CT images were post processed with 4 parameters (0%, 10%, 20% and 30%) of ASiR on a CT workstation. The volume

CT dose index ($CTDI_{vol}$) of the ATCM low dose and the standard dose CT were compared. Four experienced abdominal radiologists independently assessed the quality of the ATCM low dose CT with the aforementioned ASiR parameters using a 5-point-scale satisfaction score (1 = unacceptable, 2 = poor, 3 = average, 4 = good, and 5 = excellent image quality) by using the prior standard dose CT as a reference of an excellent image quality (5). Each reader selected the preferred ASiR parameter for each participant. The image noise of the liver and the aorta in all 5 techniques (1 prior standard dose and 4 current ATCM low dose techniques) was measured. The correlation between the image quality vs the participants' body mass index (BMI) and waist circumferences were analyzed.

Results: The mean $CTDI_{vol}$ of the ATCM low dose CT was significantly lower than of the standard dose CT (7.29 ± 0.20 vs 11.28 ± 0.23 mGy, $p<0.001$). The mean satisfaction score for the ATCM low dose CT with 0%, 10%, 20% and 30% ASiR were 4.14, 4.16, 4.17, and 4.26, respectively with the ranges of 3 to 5 in all techniques. The preferred ASiR parameters of each participant randomly selected by each reader were varied, depending on the readers' opinions. The mean image noise of the aorta on the standard dose CT and the ATCM low dose CT with 0%, 10%, 20%, and 30% ASiR was 30.69, 36.60, 34.05, 31.43, and 29.09, respectively, while the mean image noise of the liver was 24.96, 29.90, 27.86, 25.66, and 23.68, respectively. There was a correlation between the image quality (satisfaction score and image noise) vs the participants' BMI and waist circumferences.

Conclusion: The ATCM low dose CT received acceptable radiologists' satisfaction with significant radiation dose reduction. The increment of ASiR was helpful in reducing the image noise and had a tendency to increase the radiologists' satisfaction score.

Keywords: Abdominal computed tomography, Abdominal CT, Automatic tube current modulation, ATCM, Radiation dose optimization, Iterative reconstruction, IR, Adaptive statistical iterative reconstruction, ASiR.

THE ASEAN JOURNAL OF RADIOLOGY
ISSN 2672-9393

Introduction

Nowadays, many new computed tomography (CT) techniques have been proposed for the improved image quality by providing thin slice collimation and fast rotation time. In spite of getting better image resolution and ability to achieve a dynamic study, it comes with the high radiation exposure, which is considered one of the potential risks of cancer[1]. There have been many proposed techniques for radiation dose optimization, such as minimizing the number of CT acquisitions and area coverage as necessary, decreasing the tube current and the peak kilovoltage[2,3]. Automatic tube current modulation (ATCM) enables automatic adjustment of the tube current according to the size and density characteristics of the body part being scanned. It is one of the most accepted techniques for radiation dose optimization. It reduces radiation dose with an acceptable image quality as well as a fixed tube current (FTC) technique.[4-6].

However, the radiation dose reduction will inevitably increase the image noise, degrade the image quality, and disturb the image interpretation. Over the past decade, the CT vendors offered many techniques for optimizing the image quality of the low dose CT scan. One well-accepted reconstruction technique was iterative reconstruction (IR) which helped reduce the image noise compared with the conventional filtered back projection (FBP) reconstruction technique and could help diminish the radiation dose of 30-50%[7-9].

Our prior study on the abdominal CT radiation dose optimization[10] was prospectively performed in 119 participants by using the FTC technique (30% reduction of standard tube current: from 400 to be 260 mA on 64-slice CT scanner, and from 340 to be 210 mA on 256-slice CT scanner). We applied the new de-noising IR technique (Adaptive Statistical Iterative Reconstruction, ASiR) with various parameters (0%, 10%, 20%, and 30% ASiR) by post-processing on a CT workstation to improve the image quality of the low dose CT. The result of the study provided significant radiation dose reduction with an acceptable image quality.

This current phase II study was a prospective study on abdominal CT radiation dose optimization using the ATCM technique, another attractive technique for CT radiation dose optimization. The received images were also post-processed on a CT workstation with 4 parameters of ASiR (0%, 10%, 20%, and 30%). The purposes of the current study were to compare radiation dose, radiologists' satisfaction, and the image noise between the standard dose abdominal CT currently performed at our hospital and the new ATCM low dose abdominal CT, using various parameters of ASiR techniques.

Materials and methods

Study Designs and Participants

This study was a prospective, single-centered study performed at a 2,200-bed university hospital in central Thailand. This study was approved by our institutional review board with informed consents from all included participants.

All participants were aged over 18 years old who were scheduled for contrast enhanced abdominal CT examinations at our department during January 2019. They had available prior standard dose contrast enhanced abdominal CT within 180 days for comparison. In total, one hundred and eleven participants met the criteria and were recruited as our study population. The demographic data of each participant including gender, age, body mass index (BMI), and waist circumference were recorded by one of our investigators (SH).

CT Techniques

Standard Dose Abdominal CT

The prior standard dose abdominal CT of our participants was routinely performed by four General Electric (GE) CT scanners including three 64-slice scanners (one LightSpeed VCT and two Discovery CT750 High Definition, GE Healthcare, Milwaukee, WI, USA) and one 256-slice scanner (Revolution CT, GE healthcare, Milwaukee, WI, USA). The CT protocol of each participant was selected for

THE ASEAN JOURNAL OF RADIOLOGY
ISSN 2672-9393

a proper number of CT acquisitions and area coverage. All participants were advised to hold their breath during the scan. The scan coverage included at least the upper abdominal area. The slice collimation was 1.25 mm (reconstructed at 7.0 mm) for all scanners. There were varieties on the administration of oral and rectal contrasts according to each participant's appropriate protocol. All participants underwent precontrast and postcontrast studies, before and after a bolus intravenous injection of the nonionic iodinated contrast agent (2 mL per kg body weight), followed by 20 mLof water via a power injector at a rate of 3 mL/second. Each participant had at least a portovenous phase with an 80-second delay for postcontrast study. An additional arterial phase at 35 to 40-second delay or delayed phase at 5 to 10-minute delay was obtained in some participants as necessary. The peak kilovoltage was fixed at 120 kVp for all scanners. The fixed tube current based on our standard protocol was 400 mA and 340 mA for 64-slice and 256-slice CT scanners, respectively. The rotation time was 0.5 seconds for all scanners. The pitch was 1.375:1 and 0.992:1 for 64-slice and 256-slice CT scanners, respectively. All images were reconstructed with the standard FBP techniques and sent to the Picture Archiving and Communication System (PACS) for subsequent reviews.

ATCM Low Dose Abdominal CT

The ATCM low dose abdominal CT was performed by three GE CT scanners including two 64-slice scanners (Discovery CT750 High Definition, GE Healthcare, Milwaukee, WI, USA) and one 256-slice scanner (Revolution CT, GE healthcare, Milwaukee, WI, USA). Our old-fashioned 64-slice CT scanner (LightSpeed VCT, GE healthcare, Milwaukee, WI, USA) did not have the IR de-noising technique for improving the image quality; therefore, it was not included in the performance of the low dose abdominal CT. The CT scanners for the standard and low dose CT of each participant were not necessarily the same scanners. The CT protocol of each participant was selected for a proper number of CT acquisitions and area coverage (at least covering the upper abdominal area). The scan techniques were the same as described in the prior standard dose abdominal CT section except for the tube current which was automatic adjusted by the CT scanners between 150-270 mA with a fixed noise index of 18, according to the size and density characteristics of each participant's abdomen (ATCM technique).

The IR technique specific for our GE CT scanners (Adaptive Statistical Iterative Reconstruction, ASiR) was applied by blending with the conventional FBP on low dose portovenous phase images by post-processing on a CT workstation by using the 4 parameters of ASiR: 0% ASiR (with 100% FBP), 10% ASiR (with 90% FBP), 20% ASiR (with 80% FBP) and 30% ASiR (with 70% FBP). With these reconstruction techniques, four sets of low dose portovenous CT images were created and sent to PACS for subsequent reviews. We chose to study only on the portovenous phase because most abdominal organs had homogeneous enhancement on this phase. It was easy for radiologists to evaluate the CT image quality.

For a parameter of radiation dose comparison, we selected the volume CT dose index (CTDIvol) instead of dose length product (DLP). The DLP would depend on the length of scan which varied in the participants due to the difference in area coverage and the number of CT acquisitions.

The details of CT scanners, study dates, and CTDIvol of each participant's prior standard dose abdominal CT and the current ATCM low dose abdominal CT were recorded by one of our investigators (SH). The time interval between the two studies was calculated.

Image Quality Assessment

For qualitative image quality assessment, four board-certified, abdominal radiologists (PA, KM, WT, and SP with 23, 23, 17, and 17 years of experience in abdominal CT evaluation) independently reviewed one set of the standard dose portovenous abdominal CT images and 4 sets of ATCM low dose portovenous abdominal CT images with 0%, 10%, 20%, and 30% ASiR of each participant. All readers were blinded to the percentage of the applied ASiR. They graded the image quality of each low dose CT set by using a 5-point-scale satisfaction score on a visual scale as follows:

1: Unacceptable image quality, unable to interpret
2: Poor image quality, interfering with interpretation
3: Average image quality, possible interpretation
4: Good image quality
5: Excellent image quality

The satisfaction score was given by using each participant's prior standard dose CT images as a reference of an excellent image quality (5). The satisfaction scores of 3 to 5 were acceptable for CT interpretation. Each reader selected the preferred ASiR parameter from 4 sets of ATCM low dose abdominal CT for each participant.

For quantitative image quality assessment of the abdominal CT, the image noise of the aorta and the liver was measured on one set of the standard dose CT images and other 4 sets of the ATCM low dose CT images by one of our investigators (SH) on a CT workstation (Advantage workstation AW 4.6, GE healthcare, Milwaukee, WI, USA). The image noise was measured by drawing a circular region of interests (ROIs) at 4 locations (one aortic and 3 hepatic regions) on a 1.25-mm slice portovenous image at the same locations and levels of these 5 image sets. For the image noise of the aorta, the ROI was drawn at least 1/3 area of the aortic lumen (range 68-116 mm2, mean 98.48 mm2 ± 6.40 mm2) at the most central part to avoid calcified plaque at the aortic wall. For the image noise of the liver, 3 hepatic ROIs (range 74-108 mm2, mean 100.25 mm2 ± 2.69 mm2) were routinely applied on the left lobe, the anterior right lobe, and the posterior right lobes (Figure 1). In patients with prior hepatic surgery, the ROIs were placed in three different locations in the remaining hepatic areas (Figure 2). The hepatic ROIs were placed at the homogenous enhancing hepatic areas avoiding vessels, bile ducts, hepatic lesions, calcifications and surgical materials. The mean image noise of each liver was calculated from these 3 hepatic ROIs of the image noise.

Statistical Analysis

The demographic data of participants, CT scanners, time interval between CT studies, the image quality (satisfaction scores, readers' preferred ASiR parameters, image noise) and CTDIvol of the ATCM low dose and the standard dose CT were presented as number (%), mean (standard deviation, SD), median, and range. Paired t-test was used to compare mean CTDIvol between the standard dose CT and the low dose CT. Multivariate analysis with Bonferroni adjustment for a pairwise comparison was applied to compare satisfaction scores, the mean image noise of the aorta and the liver among different ASiR parameters. Spearman correlation was used to evaluate the relationship between the satisfaction score vs the participants' BMI and waist circumferences. The Pearson's correlation was used to evaluate the relationship between the image noise vs the participants' BMI and waist circumferences.

All statistical data analyses were performed by using PASW 18.0 (SPSS Inc., Chicago, IL, USA). A 2-sided p-value of less than or equal to 0.05 was considered as a statistical significance.

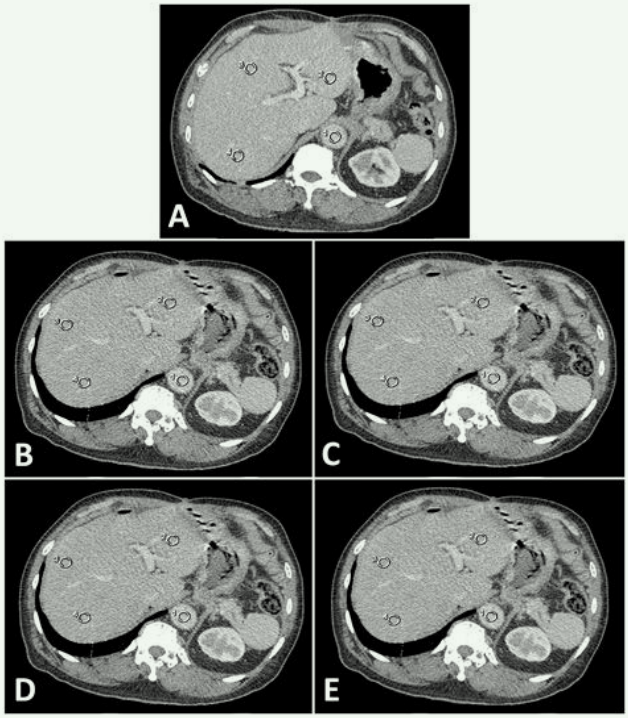

Figure 1. *The image noise measurement of the aorta (1 ROI) and the liver (3 ROIs at the left lobe, the anterior right lobe and the posterior right lobe) on the 5 image sets (A-E)*
A: Prior standard dose abdominal CT
B-E: The current ATCM low dose abdominal CT with 0% ASiR (B), 10% ASiR (C), 20% ASiR (D) and 30% ASiR (E)
The ROIs were positioned at the same locations and levels for all 5 image sets.

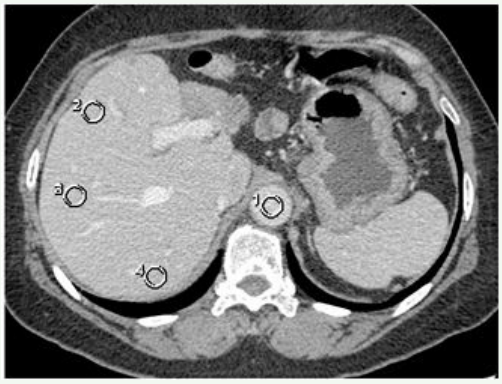

Figure 2. *In case of post left hepatectomy, the 3 hepatic ROIs were placed in three different locations in the remaining right hepatic area.*

Results

Participants

One hundred and eleven participants in this study included 63 (56.8%) men and 48 (43.2%) women. The mean age (SD) of the participants at the time of the ATCM low dose CT scan was 61.4 (12.9) years with the range of 21-95 years.

The mean BMI (SD) was 23.44 (3.89) kg/m^2 (range 16.01-34.29 kg/m^2, median 23.05 kg/m^2). With respect to BMI category, number of participants with underweight (BMI<18.5 kg/m^2), normal weight (BMI 18.5-24.9 kg/m^2), overweight (BMI 25.0-29.9 kg/m^2) and obesity (BMI ≥ 30.0 kg/m^2) were 11 (9.9%), 63 (56.8%), 30 (27.0%), and 7 (6.3%), respectively. The mean waist circumference (SD) was 84.4 (9.2) cm (range 66-113 cm, median 83 cm).

CT Techniques

The standard dose abdominal CT of 72 (64.9%) and 39 (35.1%) participants were performed by 64-slice and 256-slice scanners, respectively. The ATCM low dose abdominal CT of 65 (58.6%) and 46 (41.4%) participants were performed by 64-slice and 256-slice scanners, respectively. The time interval between the two studies ranged from 13 to 178 days (median 132 days).

The mean $CTDI_{vol}$ (SD) of the ATCM low dose CT was significantly lower than that of standard dose CT, 7.29 (0.20) vs 11.28 (0.23) mGy ($p<0.001$).

Image Quality Assessment

For qualitative image quality assessment, the satisfaction score of the ATCM low dose abdominal CT with 4 ASiR parameters graded by 4 readers ranged from 3 to 5, which were all acceptable for CT interpretation. The mean satisfaction scores of the ATCM low dose abdominal CT with 4 ASiR parameters were summarized in Table 1. The preferred ASiR parameters applied to the low dose CT of each participant was randomly selected by each reader, displayed in Table 2.

For quantitative image quality assessment, the image noise of the aorta and the liver on the standard dose CT and the ATCM low dose CT with 4 ASiR parameters was summarized in Table 3 and 4 (Figure 3 and 4). As expected, the ATCM low dose CT had a higher image noise of the aorta and the liver than the standard dose CT. After applying the ASiR technique, the image noise on the low dose CT images decreased. The higher percentage of ASiR employed, the lower image noise of the aorta and the liver was obtained.

There was a correlation between the image quality (satisfaction score and image noise) vs the participants' BMI and waist circumferences. Patients with high BMI and large waist circumferences received lower satisfaction scores and had more image noises on their CT images. The correlation of the image quality vs BMI was stronger than vs waist circumference (Table 5 and 6).

Table 1. *The mean satisfaction scores of the ATCM low dose abdominal CT with 0%, 10%, 20%, and 30% ASiR parameter graded by 4 readers.*

	Mean Satisfaction Scores (SD) of ATCM Low Dose Abdominal CT			
	0% ASiR	10% ASiR	20% ASiR	30% ASiR
Reader 1	4.53 (0.52)	4.53 (0.54)	4.50 (0.52)	4.50 (0.54)
Reader 2	3.24 (0.43)	3.33 (0.47)	3.39 (0.49)	3.74 (0.44)
Reader 3	4.19 (0.72)	4.18 (0.72)	4.19 (0.71)	4.23 (0.71)
Reader 4	4.61 (0.49)	4.60 (0.49)	4.60 (0.49)	4.56 (0.50)
All readers	4.14 (0.40)	4.16 (0.41)	4.17 (0.40)	4.26 (0.39)

Note: There were significant statistical differences between
0% ASiR vs 30% ASiR ($p<0.001$); 95%CI (0.062, 0.163)
10% ASiR vs 30% ASiR ($p<0.001$); 95%CI (0.043, 0.146)
20% ASiR vs 30% ASiR ($p<0.001$); 95%CI (0.038, 0.133)

Table 2. *The preferred ASiR parameters applied to the ATCM low dose abdominal CT selected by 4 readers.*

	Number of The Preferred ASiR Parameter (%)				
	0% ASiR	10% ASiR	20% ASiR	30% ASiR	Total
Reader 1	48 (43.2)	33 (29.7)	21 (18.9)	9 (8.1)	111 (100.0)
Reader 2	7 (6.3)	9 (8.1)	19 (17.1)	76 (68.5)	111 (100.0)
Reader 3	3 (2.7)	15 (13.5)	28 (25.2)	65 (58.6)	111 (100.0)
Reader 4	68 (61.3)	26 (23.4)	9 (8.1)	8 (7.2)	111 (100.0)

Table 3. *The image noise of the aorta and the liver on standard dose CT and ATCM low dose CT with 4 different ASiR parameters.*

	Standard Dose CT	ATCM Low Dose CT			
		0% ASiR	10% ASiR	20% ASiR	30% ASiR
Aorta					
Mean (SD)	30.69 (6.39)	36.60 (6.33)	34.05 (6.06)	31.43 (5.70)	29.09 (5.43)
Min	17.43	22.84	21.56	19.80	18.28
Max	47.50	56.20	53.67	50.47	47.93
Liver					
Mean (SD)	24.96 (5.62)	29.90 (5.63)	27.86 (5.08)	25.66 (4.65)	23.68 (4.35)
Min	13.90	17.18	15.73	14.64	13.47
Max	41.68	46.48	43.33	40.49	37.70

Table 4. *The differences of the mean image noise of the aorta and the liver on the ATCM low dose CT with 4 different ASiR parameters compared to the standard dose CT.*

	Differences (SD) of Mean Image Noise of Low Dose CT Compared to Standard Dose CT	p-Value	95% CI
Aorta			
0% ASiR	5.91 (0.57)	<0.001	4.28, 7.56
10% ASiR	3.36 (0.56)	<0.001	1.75, 4.98
20% ASiR	0.74 (0.58)	1.000	-0.91, 2.39
30% ASiR	-1.60 (0.57)	0.059	-3.22, 0.03
Liver			
0% ASiR	4.94 (0.34)	<0.001	3.96, 5.92
10% ASiR	2.90 (0.33)	<0.001	1.95, 3.86
20% ASiR	0.70 (0.34)	0.400	-0.26, 1.66
30% ASiR	-1.28 (0.34)	0.003	-2.26, -0.30

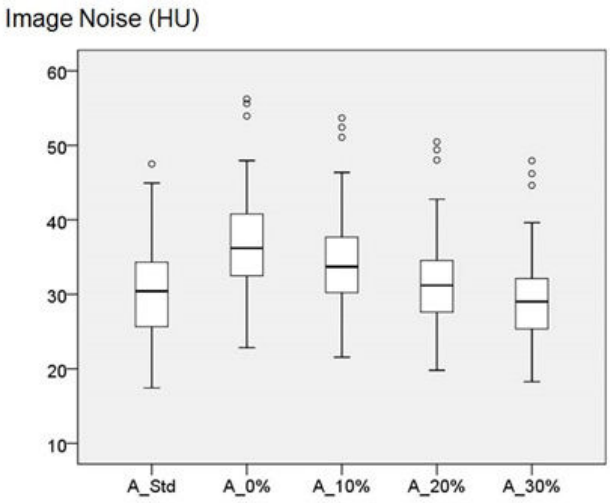

Figure 3. *The graph shows the mean image noise (range) of the aorta on the standard dose CT (A_std) and the ATCM low dose CT with 0% ASiR (A_0%), 10% ASiR (A_10%), 20% ASiR (A_20%) and 30% ASiR (A_30%).*

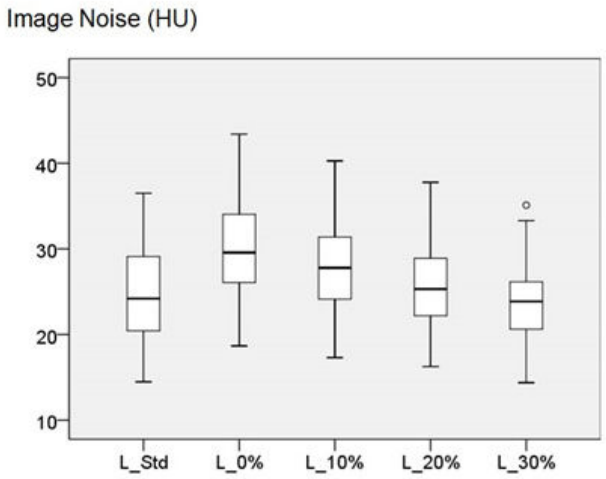

Figure 4. *The graph shows the mean image noise (range) of the liver on the standard dose CT (L_std) and the ATCM low dose CT with 0% ASiR (L_0%), 10% ASiR (L_10%), 20% ASiR (L_20%) and 30% ASiR (L_30%).*

Table 5. *The correlation between satisfaction score vs BMI and waist circumference on the standard dose CT and the low dose CT with different ASiR parameters.*

	BMI		Waist Circumference	
	R	p-Value	R	p-Value
0% ASIR	-0.333	<0.001	-0.222	0.19
10% ASIR	-0.364	<0.001	-0.229	0.16
20% ASIR	-0326	<0.001	-0.204	0.32
30% ASIR	-0.313	=0.001	-0.192	0.43

Table 6. *The correlation between the image noise of the aorta and the liver vs BMI and waist circumference on the standard dose CT and the low dose CT with different ASiR parameters.*

	BMI		Waist Circumference	
	R	p-Value	R	p-Value
Aorta				
Standard	0.633	<0.001	0.599	<0.001
0% ASIR	0.516	<0.001	0.475	<0.001
10% ASIR	0.504	<0.001	0.475	<0.001
20% ASIR	0.471	<0.001	0.459	<0.001
30% ASIR	0.470	<0.001	0.480	<0.001
Liver				
Standard	0.737	<0.001	0.646	<0.001
0% ASIR	0.729	<0.001	0.610	<0.001
10% ASIR	0.690	<0.001	0.584	<0.001
20% ASIR	0.700	<0.001	0.594	<0.001
30% ASIR	0.671	<0.001	0.585	<0.001

THE ASEAN JOURNAL OF RADIOLOGY
ISSN 2672-9393

Discussion

With the worldwide concern about radiation safety, there have been several novel CT reconstruction techniques to enhance the image quality, allowing the radiologists to continue reducing the CT radiation dose for the sake of patient's safety while still accomplishing the satisfactory image quality. The IR is one of the new image reconstruction techniques that have been developed in the past decade. Previous studies assessing the imaging quality obtained from the low dose CT with the IR techniques reported that the IR technique helped improve the image quality by decreasing the image noise and provided a comparable image quality as the standard dose CT[11-13].

At our hospital, we used ASiR (IR technique specific for our GE CT scanners) to blend with the conventional FBP technique to optimize the image quality of the low dose CT. As a result of our study, the ATCM low dose abdominal CT significantly reduced the radiation dose compared to the standard dose abdominal CT. The image quality of all low dose techniques was acceptable for interpretation, although the image noise was significantly increased in 0% ASiR and 10% ASiR image sets. When applying 20% and 30% ASiR to the ATCM low dose abdominal CT images, there was no significant difference of the image noise of the aorta and the liver compared to the standard dose CT. Our results were similar to several prior studies[10-16].

Our study showed that the mean satisfaction score had a tendency to increase when the higher percentage ASiR applied. The 30% ASiR image set showed a significantly higher satisfaction score compared to other low dose image sets. For the preferred image set, there were different opinions between 4 readers. Two readers preferred the lower percentage of ASiR, while the other two readers preferred the higher percentage of ASiR. We assumed that the images with the high percentage of ASiR provided smooth image appearances with less sharp borders. This was the reported major drawback of the IR technique[11,13]. Some of our readers were possibly familiar with a relatively noisy image with sharp borders derived from the conventional FBP technique.

Our study showed the correlation between the image quality (satisfaction score and image noise) vs the participants' BMI and waist circumferences. Patients with high BMI or large waist circumferences received lower satisfaction scores and had more image noises on their CT images. After applying ASiR, it helped improve the image quality in patients with high BMI and large waist circumference. Shaqdan et al.[17] supported the result of our study. They reported that IR provided a significantly higher image quality (less image noise and higher contrast-to-noise ratio) compared to the FBP reconstruction technique in obese patients.

This current study was designed to diminish the limitations of our phase I study [10]. Reviewers in this current study were blinded to the percentage of ASiR applied to ATCM low dose CT images; and the time interval between the standard dose and the ATCM low dose CT was limited within 180 days. We found that either FTC (phase I study) or ATCM (the current study) low dose CT with ASiR provided an acceptable image quality and significant radiation dose reduction compared with standard dose CT. From our experience, the FTC technique is simple and easy to be performed, while ATCM is more complicated, requires technicians with more expertise. A direct comparison between FTC and ATCM should be further studied for more accurate information.

With the attempt to reduce the radiation dose for the sake of patient's safety, the image quality is inevitably decreased although many novel reconstruction techniques are applied. Radiologists should realize the importance of radiation optimization and open their mind to adopt low dose CT images with an acceptable image quality. Radiologists are the key people to balance the amount of radiation dose reduction and the suitable image quality for accurate CT interpretation.

There were several limitations of our study. First, there were variables in our CT scanners. Although they were all GE scanners, most were 64-slice scanners and one was a 256-slice scanner. Of which, some CT parameters (i.e. mA and pitch) were not the same. Inherent differences in scanners could affect the results of the study. Plus, the CT scanners for the standard and the low dose CT of each participant were not necessarily the same scanners. Second, the time interval

THE ASEAN JOURNAL OF RADIOLOGY
ISSN 2672-9393

between the prior standard dose CT and the current low dose CT ranged from 13 to 178 days (median 132 days). Although shorter than 6 months, there could be any changes in participants' habitus or conditions that could affect the image quality. The new study with a shorter time interval should be designed. Third, the image noise was measured on a 1.25 mm slice portovenous image of each image set. Actually, the image noise should be measured by choosing 3-5 consecutive CT slices and the noise should be averaged for the statistical accuracy. Finally, our study focused only on the image quality (satisfaction score and image noise) of the low dose CT. We did not study diagnostic performances of the low dose CT. To evaluate the diagnostic performances between the low dose CT and the standard dose CT, these 2 studies should be performed on the same date and in almost the same acquisition phase. These will inevitably increase the radiation dose received by the participants.

In conclusion, the ATCM low dose CT with the tube current between 150 and 270 mA and a fixed noise index of 18 received acceptable radiologists' satisfaction with significant radiation dose reduction. The increment of ASiR technique was helpful in reducing the image noise and had a tendency to increase the radiologists' satisfaction score.

References

1. Hall EJ, Brenner DJ. Cancer risks from diagnostic radiology: the impact of new epidemiological data. Br J Radiol 2012;85:e1316-7. doi: 10.1259/bjr/13739950.

2. Hara AK, Wellnitz CV, Paden RG, Pavlicek W, Sahani DV. Reducing body CT radiation dose: beyond just changing the numbers. AJR Am J Roentgenol 2013;201:33-40. doi: 10.2214/AJR.13.10556.

3. Tamm EP, Rong XJ, Cody DD, Ernst RD, Fitzgerald NE, Kundra V. Quality initiatives: CT radiation dose reduction: how to implement change without sacrificing diagnostic quality. Radiographic 2011;31:1823-32. doi: 10.1148/rg.317115027.

4. Kalra MK, Maher MM, Toth TL, Schmidt B, Westerman BL, Morgan HT, et al. Techniques and applications of automatic tube current modulation for CT. Radiology 2004;233:649-57. doi: 10.1148/radiol.2333031150.

5. Kalra MK, Maher MM, Toth TL, Kamath RS, Halpern EF, Saini S. Comparison of Z-axis automatic tube current modulation technique with fixed tube current CT scanning of abdomen and pelvis. Radiology 2004;232:347-53. doi: 10.1148/radiol.2322031304.

6. Lee S, Yoon SW, Yoo SM, Ji YG, Kim KA, Kim SH, et al. Comparison of image quality and radiation dose between combined automatic tube current modulation and fixed tube current technique in CT of abdomen and pelvis. Acta Radiol 2011;52:1101-6. doi: 10.1258/ar.2011.100295.

7. Patino M, Fuentes JM, Singh S, Hahn PF, Sahani DV. Iterative reconstruction techniques in abdominopelvic CT: Technical concepts and clinical implementation. AJR Am J Roentgenol 2015;205:W19-31. doi: 10.2214/AJR.14.13402.

THE ASEAN JOURNAL OF RADIOLOGY
ISSN 2672-9393

8. Willemink MJ, de Jong PA, Leiner T, de Heer LM, Nievelstein RA, Budde RP, et al. Iterative reconstruction techniques for computed tomography Part 1: technical principles. Eur Radiol 2013;23:1623-31. doi: 10.1007/s00330-012-2765-y.

9. Geyer LL, Schoepf UJ, Meinel FG, Nance JW Jr, Bastarrika G, Leipsic JA, et al. State of the art: iterative CT reconstruction techniques. Radiology 2015;276: 339-57. doi: 10.1148/radiol.2015132766.

10. Apisarnthanrak P, Buranont C, Boonma C, Janpanich S, Suwatananonthakij T, Klinhom A, et al. Abdominal CT radiation dose optimization at Siriraj Hospital. ASEAN J Radiol 2020;21:28-43.

11. Mitsumori LM, Shuman WP, Busey JM, Kolokythas O, Koprowicz KM. Adaptive statistical iterative reconstruction versus filtered back projection in the same patient: 64 channel liver CT image quality and patient radiation dose. Eur Radiol 2012;22:138-43. doi: 10.1007/s00330-011-2186-3.

12. Prakash P, Kalra MK, Kambadakone AK, Pien H, Hsieh J, Blake MA, et al. Reducing abdominal CT radiation dose with adaptive statistical iterative reconstruction technique. Invest Radiol 2010;45:202-10. doi: 10.1097/RLI.ob013e3181dzfeec.

13. Sagara Y, Hara AK, Pavlicek W, Silva AC, Paden RG, Wu Q. Abdominal CT: comparison of low-dose CT with adaptive statistical iterative reconstruction and routine-dose CT with filtered back projection in 53 patients. AJR Am J Roentgenol 2010;195:713-9. doi: 10.2214/AJR.09.2989.

14. Willemink MJ, Takx RA, de Jong PA, Budde RP, Bleys RL, Das M, et al. Computed tomography radiation dose reduction: effect of different iterative reconstruction algorithms on image quality. J Comput Assist Tomogr 2014;38:815-23. doi: 10.1097/RCT.0000000000000128.

15. Gervaise A, Osemont B, Louis M, Lecocq S, Teixeira P, Blum A. Standard dose versus low-dose abdominal and pelvic CT: comparison between filtered back projection versus adaptive iterative dose reduction 3D. Diagn Interv Imaging 2014;95:47-53. doi: 10.1016/j.diii.2013.05.005.

16. Singh S, Kalra MK, Shenoy-Bhangle AS, Saini A, Gervais DA, Westra SJ, et al. Radiation dose reduction with hybrid iterative reconstruction for pediatric CT. Radiology 2012;263:537-46. doi: 10.1148/radiol.12110268.

17. Shaqdan KW, Kambadakone AR, Hahn P, Sahani DV. Experience with iterative reconstruction techniques for abdominopelvic computed tomography in morbidly and super obese patients. J Comput Assist Tomogr 2018;42:124-32. doi: 10.1097/RCT.0000000000000656.

THE ASEAN JOURNAL OF RADIOLOGY
ISSN 2672-9393

Clinico-Radiologic-Pathologic Correlation

Imaging appearance of the involved mesenteric node in patient with systemic amyloidosis: A case report

Sunpob Cheewadhanaraks, M.D.[(1)]
Thitithep Suriyamonthon, M.D.[(1)]
Paramee Noisri, M.D.[(1)]
Pimporn Puttawibul, M.D.[(1)]
Tanawat Pattarapuntakul, M.D.[(2)]
Naruemon Wisedopas, M.D.[(3)]
Pakorn Arunsawat, M.D.[(4)]
Khanin Khanungwanitkul, M.D.[(1)]

From [(1)]Department of Radiology, Faculty of Medicine, Prince of Songkla University, Songkhla, Thailand.
[(2)]Department of Internal Medicine, Faculty of Medicine, Prince of Songkla University, Songkhla, Thailand.
[(3)] Department of Pathology, Faculty of Medicine, Chulalongkorn University, Bangkok, Thailand.
[(4)] Anatomical pathology unit, Hatyai Hospital, Songkhla, Thailand.

Address correspondence to K.K. (e-mail: khanin14@gmail.com)

Received 8 December 2020; revised 15 December 2020; accepted 16 December 2020
doi:10.46475/aseanjr.v21i3.98

Abstract

Amyloidosis is a rare disease characterised by abnormal amyloid protein deposition within the affected tissue. About 37% of the patients were presented with systemic amyloidosis, of which hilar, mediastinal, and para-aortic lymph nodes were involved. Deposition of amyloid protein in the mesenteric lymph node is rarely documented, but when reported, it is seen in isolated or secondary amyloidosis. Despite an indistinguishable imaging appearance of the amyloid-deposit mesenteric node from malignancy, infection, and an inflammation process, the radiologists should be aware of variable imaging findings to be suspicious of amyloidosis. We reported a rare case of systemic amyloidosis with mesenteric node involvement, manifested as node enlargement.

Keywords: Amyloidosis, Mesenteric, Lymph node, Imaging findings, Clinical presentation.

Introduction

Amyloidosis is a rare group of disease defined by extracellular deposition and accumulation of abnormal proteins called amyloid. The most common form of this rare disease is systemic amyloidosis which is about 80-90% of all patients. Systemic amyloidosis can be classified into two groups based on biochemical structure of amyloid fibrils: primary amyloidosis (AL-amyloidosis) and secondary amyloidosis (AA-amyloidosis). AL-amyloidosis has a propensity to be associated with plasma cell disorders, especially multiple myeloma and monoclonal gammopathy. On the other hand, AA-amyloidosis is generally a result of infection or an inflammatory process such as osteomyelitis, granulomatous infection, connective tissue diseases, and neoplasms[1,2].

An imaging appearance of systemic amyloidosis can be varied and involve many organ systems such as cardiopulmonary, gastrointestinal, genitourinary, and musculoskeletal systems[3]. Additionally, lymph node involvement is not uncommon; about 37% of the patients demonstrated hilar, mediastinal, and para-aortic adenopathy[4]. On the contrary, the involvement of the mesenteric lymph node by amyloidosis is rather rare and seldom documented[5-6].

In this article, we would like to share a case report of systemic amyloidosis with pathologically proven mesenteric node involvement, which was accidentally revealed when the patient was referred for chronic diarrhea evaluation. Additionally, we also review a few case reports which published quite similar imaging appearances of this rare manifestation.

THE ASEAN JOURNAL OF RADIOLOGY
ISSN 2672-9393

Case summary

A 33-year-old woman, with an underlying hemoglobin E-beta thalassemia trait, was presented to the hospital with paraumbilical pain and chronic watery diarrhea, a large number of feces, about 500-1,000 mL each time without blood or mucous. The frequency is 4-5 times per day, for 3 months. Her vital signs were unremarkable. The physical examination showed pale conjunctiva, a distended abdomen with tympanic on percussion and a hyperactive bowel sound without tenderness, nor a palpable mass. The laboratory results showed mild anemia (Hb 9.3 g/dL, Hct 30.1%), hypoalbuminemia /hypogloglobuminemia (Alb 1.69 g/dL, Globulin 2.1 g/dL), hypokalemia and hyponatremia. The stool examination and stool acid fast strain were unremarkable. The initial bedside abdominal ultrasonography revealed a 5.3-cm intraabdominal mass below the umbilicus. Therefore, subsequent computed tomography (CT) of the whole abdomen was performed (Figure 1).

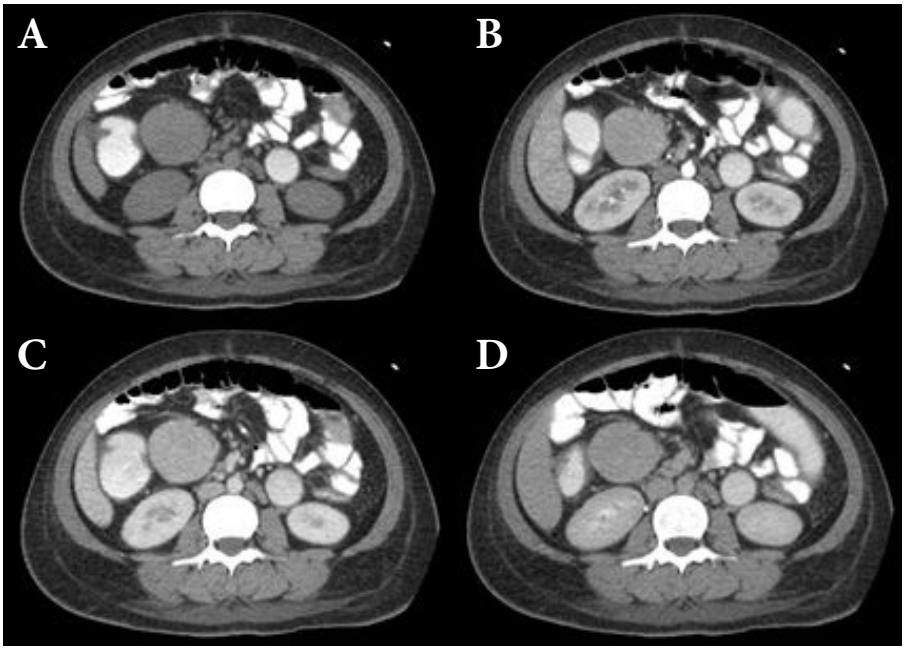

Figure 1. *CT whole abdomen in plain (A), arterial (B), venous (C) and delayed (D) phases at 5 minutes shows a well-defined homogeneous mass with moderate enhancement at the right side of the mid abdomen. No intralesional calcification or necrosis is found.*

Imaging, endoscopic, and pathologic findings

She was admitted for supportive treatment and additional colonoscopy and esophagogastroduodenoscopy (EGD). The colonoscope was passed up to 10 cm from the ileocecal valve, which revealed ileitis and multiple small erosions. The EGD also showed diffuse erythematous mucosa without an ulcer along the stomach, duodenum, jejunum, and ileum. No obvious intraluminal mass was found along the gastrointestinal tract. She was treated as having colitis with intravenous antibiotics for 7 days. Then she was discharged after her clinical condition had been minimally improved.

However, after a few weeks, she was re-admitted due to acute paraumbilical pain with persistent chronic watery diarrhea and malnutrition. The physical examination still showed pale conjunctiva and mild tender at an umbilical area. Persistent hypoalbuminemia and diarrhea were suggestive of protein losing enteropathy. The technetium-99m human serum albumin abdominal scintigraphy was then performed (Figure 2). The result showed extravasation of the radiopharmaceuticals into the small bowel which confirmed protein losing enteropathy.

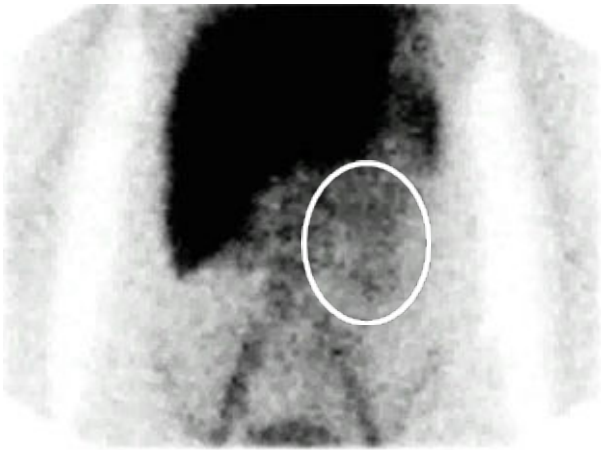

Figure 2. *Abdominal scintigraphy was performed by dynamic study at 1 hour after injection of Technetium-99m labeled to human serum albumin (^{99m}Tc-HSA). There is extravasation of radionuclides to the small bowel in the left upper quadrant with peristalsis in the dynamic study (white circle). Protein losing enteropathy at the small bowel area was suspected by this study.*

The follow-up CT of the whole abdomen showed insignificant change in size of the mass. Later on, the patient was scheduled for laparoscopic mesenteric mass resection. After the removal of the mass, the microscopic examination was performed (Figure 3). The result exhibited amyloid deposits in the mesenteric lymph node, which were confirmed by apple-green birefringence under polarised light on Congo-red stain. The patient was diagnosed to have amyloidosis.

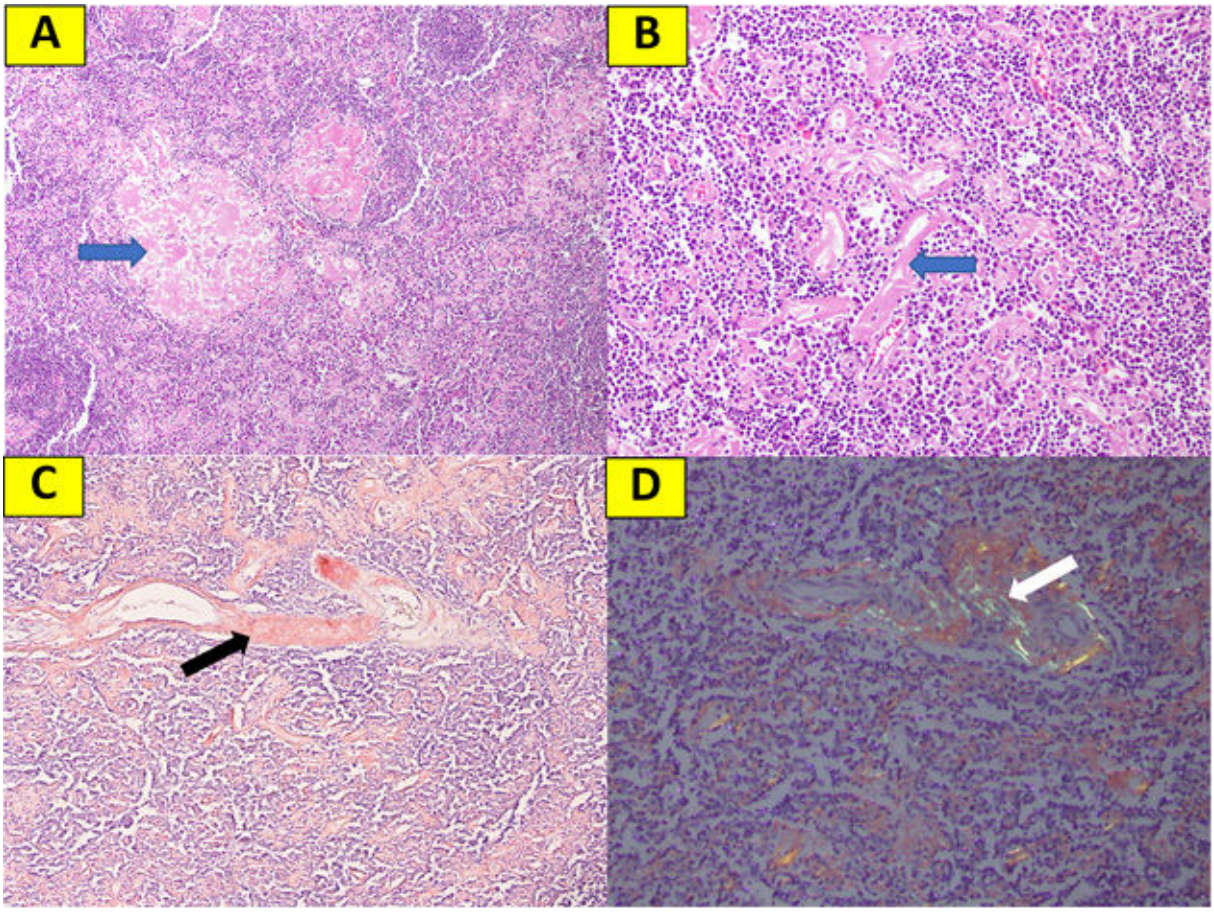

Figure 3. *The microscopic examination of mesenteric mass resection demonstrated (A and B) abundant deposits of pink amorphous material (blue arrow) within the lymphoid tissue (Hematoxylin and Eosin); (C) amyloid deposits were confirmed by a positive Congo red stain, which revealed the characteristic salmon-pink color (black arrow) (Congo red); and (D) amyloid deposits exhibited characteristic apple-green birefringence under polarised light (white arrow) (Congo red under polarised light).*

Additional laboratory investigation including bone marrow biopsy, serum immunoelectrophoresis, and immunoglobulin free light chain were performed but all studies showed unremarkable results. However, the serum beta-2 microglobulin (B2M) was high. As a result, AA-amyloidosis is suggested as a final diagnosis rather than AL-amyloidosis.

After the mesenteric mass was removed by surgical excision, she was significantly improved in both watery diarrhea and malnutrition (anemia and edema). During the six-month follow-up after the surgery, she admittedly felt well and gained some weight. No additional treatment was given.

Discussion

Amyloidosis is a constellation of disease entities defined by extracellular deposition and accumulation of abnormal proteins called amyloid. The most common form is systemic amyloidosis, which could be either primary or secondary[1]. While hilar, mediastinal, and para-aortic nodes are commonly affected by this disease, the involvement of the mesenteric node is unarguably rare[4-6].

A few case reports, of which mesenteric nodes were involved, have claimed that amyloidosis-inflicted lymph nodes may contain intralesional calcification[4,7,8]. A recent case report by Bernabei et al.[8] revealed secondary amyloidosis associated with Castleman disease, which manifested as a large calcified mesenteric mass. Hiller at el. also claimed that internal punctate calcification can be found in 50% of amyloidosis-inflicted lymph nodes.

However, in our case with secondary amyloidosis, the involved mesenteric node was observed as a well-defined homogeneously enhanced mass without intralesional calcification. Bhavsar et al.[9] also published a case report of primary amyloidosis with multiple well-defined mesenteric masses showing homogeneously enhancement and absence of internal calcification, similar to our case.

THE ASEAN JOURNAL OF RADIOLOGY
ISSN 2672-9393

Therefore, we conclude that imaging features of lymph nodes are non-specific, whether they contain intralesional calcifications or not. If there is no intralesional calcification, the differential diagnosis includes hematologic malignancy, metastasis, infection, and an inflammatory process. Under different circumstances with intralesional calcification, the differential diagnosis includes ovarian cancer, granulomatous infection, primary carcinoid tumor, lymphoma after chemotherapy, and sclerosing mesenteritis[10].

Eventually, definite diagnosis by histology is required. The positive result is seen as an appearance of classic apple-green color birefringence under the polarised light, after staining the tissue with Congo red[11].

Conclusion

Mesenteric node involvement by systemic amyloidosis, manifested as an enlarged node, is rare but possible, as in our case and a few other case reports. Intralesional calcification could be a helpful feature for suggesting amyloidosis. When the intralesional calcification is absent, the radiologists should still be aware of variable imaging findings and possibility of amyloidosis. However, histological confirmation is unquestionably required for definite diagnosis.

References

1. Ozcan HN, Haliloglu M, Sokmensuer C, Akata D, Ozmen M, Karcaaltincaba M. Imaging for abdominal involvement in amyloidosis. Diagn Interv Radiol 2017;23:282-5. doi: 10.5152/dir.2017.16484.

2. Scott PP, Scott WW Jr, Siegelman SS. Amyloidosis: an overview. Semin Roentgenol 1986;21:103-12. doi: 10.1016/0037-198x(86)90027-1.

3. Georgiades CS, Neyman EG, Barish MA, Fishman EK. Amyloidosis: review and CT manifestations. Radiographics 2004;24:405-16. doi: 10.1148/rg.242035114.

4. Vanhoenacker FM, Vanwambeke K, Jacomen G. Amyloidosis: an unusual cause of mesenteric, omental and lymph node calcifications. JBR-BTR 2014;97:283-6. doi: 10.5334/jbr-btr.1329.

5. Mohan V, Kemp JA, Lewine HE, Rabin M, Goldstein ML, Farraye FA. Diffuse mesenteric amyloidosis. Dig Dis Sci 1997;42:1079–82. doi: 10.1023/a:1018809724577.

6. Glynn TP Jr, Kreipke DL, Irons JM. Amyloidosis: diffuse involvement of the retroperitoneum. Radiology 1989;170(3 Pt1):726. doi: 10.1148/radiology.170.3.2916026.

7. Bernabei L, Waxman A, Caponetti G, Fajgenbaum DC, Weiss BM. AA amyloidosis associated with Castleman disease. Medicine(Baltimore) 2020; 99: e18978. doi: 10.1097/MD.0000000000018978.

8. Hiller N, Fisher D, Shmesh O, Gottschalk-Sabag S, Dolberg M. Primary amyloidosis presenting as isolated mediastinal mass: diagnosis by fine needle biopsy. Thorax 1995;50:908–9. doi: 10.1136/thx.50.8.908.

THE ASEAN JOURNAL OF RADIOLOGY
ISSN 2672-9393

9. Bhavsar T, Vincent G, Durra H, Khurana JS, Huang Y. Primary amyloidosis involving mesenteric lymph nodes: diagnosis by fine-needle aspiration cytology. Acta Cytol 2011;55:296-301. doi: 10.1159/000324181.

10. Sheth S, Horton KM, Garland MR, Fishman EK. Mesenteric neoplasms: CT appearances of primary and secondary tumors and differential diagnosis. Radiographics 2003;23:457-73. doi: 10.1148/rg.232025081.

11. Howie AG, Brewer DB, Howell D, Jones AP. Physical basis of colors seen in Congo red-stained amyloid in polarised light. Lab Invest 2008;88:232-42. doi: 10.1038/labinvest.3700714.

Classic Case

Imaging features of pulmonary involvement in a case of systemic amyloidosis: A classic case

Pattharapong Saneha, M.D.
Thanarak Thongsuk, M.D.
Laksika Bhuthathorn, M.D.
From Department of Radiology, Faculty of Medicine, Prince of Songkhla University, Songkhla, Thailand
Address correspondence to P.S. (e-mail: peetpat34@gmail.com)

Received 8 December 2020; revised 15 December 2020; accepted 16 December 2020
doi:10.46475/aseanjr.v21i3.99

Abstract

Amyloidosis is a disease caused by pathologic extracellular deposition of abnormal insoluble proteins throughout the body[1]. Pulmonary amyloidosis is a form of amyloid deposition confined in the lung parenchyma and may cause airway obstruction, dysphagia, and chronic pleural effusions, often with nonspecific chest imaging findings[1,2].

A 56-year-old male with underlying light chain multiple myeloma and systemic amyloidosis presented with fever for two days without dyspnoea or cough. Further chest imaging revealed nonspecific findings including consolidations, ground-glass opacities, interlobular septal thickening in both upper lobes, and bilateral pleural effusions; a diagnosis of pneumonia with pulmonary oedema was made. After the patient failed to respond to treatment, bronchoscopy with tissue biopsy was performed for unresolving pneumonia. Histopathological results were consistent with pulmonary amyloidosis.

Keywords: Pulmonary amyloidosis, Systemic amyloidosis, Multiple myeloma.

THE ASEAN JOURNAL OF RADIOLOGY
ISSN 2672-9393

Introduction

Amyloidosis is a rare disease caused by pathologic extracellular deposition of abnormal insoluble proteins throughout the body[1]. Pathogenesis of amyloidosis is characterised by protein misfolding disorders, resulting in accumulation and aggregation of this nonfunctional and toxic protein which causes damage to cells and tissues[3]. The disease may be classified as a primary or secondary disease, with primary amyloidosis being more common. Secondary amyloidosis may be caused by a variety of pathologic processes such as chronic infection, inflammation, or underlying malignancies[1].

Amyloidosis involves various organs including lungs, heart, kidneys, liver, soft tissues, the peripheral and/or autonomic nervous system, and the gastrointestinal tract[4]. The clinical symptoms of pulmonary amyloidosis may range from asymptomatic to nonspecific symptoms such as progressive dyspnoea, cough, wheezing, and respiratory failure[5].

Pulmonary involvement of amyloidosis may manifest as nodular parenchymal and diffuse alveolar septal forms, both of which have nonspecific radiological findings. Imaging findings of nodular parenchymal amyloidosis includes solitary or multiple pulmonary nodules which may, albeit rarely, calcify and cavitate[1]. These findings mimic a variety of other diseases, including granulomatous infections and malignancies, making a diagnosis based on imaging findings alone challenging and biopsy is often required for a definitive diagnosis.

Diffuse alveolar septal amyloidosis is less commonly found, but more clinically important as patients usually have a far worse prognosis compared to a nodular parenchymal subtype and are more likely to develop pulmonary hypertension and respiratory failure. Imaging findings of diffuse alveolar septal amyloidosis includes reticulonodular opacities, interlobar septal thickening, and confluent consolidations with basal and peripheral predominance[1].

Pleural involvement of amyloidosis most commonly manifests as pleural effusions, and airway involvement may manifest as long-segment submucosal plaques in the airways[1]. Pulmonary amyloidosis may cause airway obstruction, dysphagia, and chronic pleural effusions[2].

In this article, we present a classic case of pulmonary amyloidosis manifesting as nonspecific radiological findings of the chest in a case initially diagnosed with pneumonia, but subsequently diagnosed pulmonary amyloidosis through bronchoscopy with tissue biopsy performed for unresolving pneumonia.

Case Summary

A 56-year-old man with underlying International Staging System (ISS) stage II light chain multiple myeloma, biopsy-proven systemic amyloidosis, and MRI-proven cardiac amyloidosis, presented with fever for two days without dyspnoea or cough. Physical examination reveals that the patient had a fever, hypotension, and tachypnoea. An examination of the lungs revealed bilateral diffuse crepitation. Laboratory results showed mild anaemia (Hemoglobin 9.1 g/dl, Hematocrit 27.8%), with normal white blood cell and platelet counts. His chest radiograph reveals diffuse patchy opacification with air bronchogram in both lungs, predominantly in both upper lobes (figure 1).

The initial problem list included pneumonia with septic shock in an immunocompromised host, suspected pulmonary oedema, and his underlying medical conditions. A provisional diagnosis of bacterial pneumonia was made, while differential diagnoses included opportunistic infections such as *Pneumocystis jiroveci* pneumonia (PJP), pulmonary tuberculosis, and other fungal infections. He was admitted for antibiotic treatment and further laboratory investigations.

THE ASEAN JOURNAL OF RADIOLOGY
ISSN 2672-9393

Sputum cultures found *Pseudomonas aeruginosa*, and the PCR test was positive for *Pneumocystis jiroveci*; a diagnosis of bacterial pneumonia and PJP was made. After initial treatment with antibiotics and diuretics, the patient's clinical symptoms failed to improve and further diagnostic bronchoscopy for evaluation of unresolving pneumonia was indicated.

A venous phase chest computed tomography (CT) was performed for preprocedural evaluation prior to bronchoscopy by the pulmonologist. The patient's chest CT showed consolidations, ground-glass opacities, and interlobular septal thickening, predominantly in both upper lobes (figure 2). Bilateral pleural effusions were also detected. These nonspecific imaging findings support both diagnoses of pneumonia and pulmonary oedema and the patient underwent diagnostic bronchoscopy as planned.

Bronchoscopy revealed normal bronchi without endotracheal mass, and bronchoalveolar lavage with transbronchial tissue biopsy of the posterior segment of the right upper lobe was done. Histological examination revealed interstitial thickening with deposition of pink amorphous material. Congo red stain revealed apple-green birefringence in polarised light (figure 3); findings were consistent with amyloid deposits. The patient was therefore diagnosed with pulmonary amyloidosis.

After further treatment with antibiotics and diuretics, the patient's clinical condition slowly improved, and he was subsequently discharged with antibiotics for PJP prophylaxis.

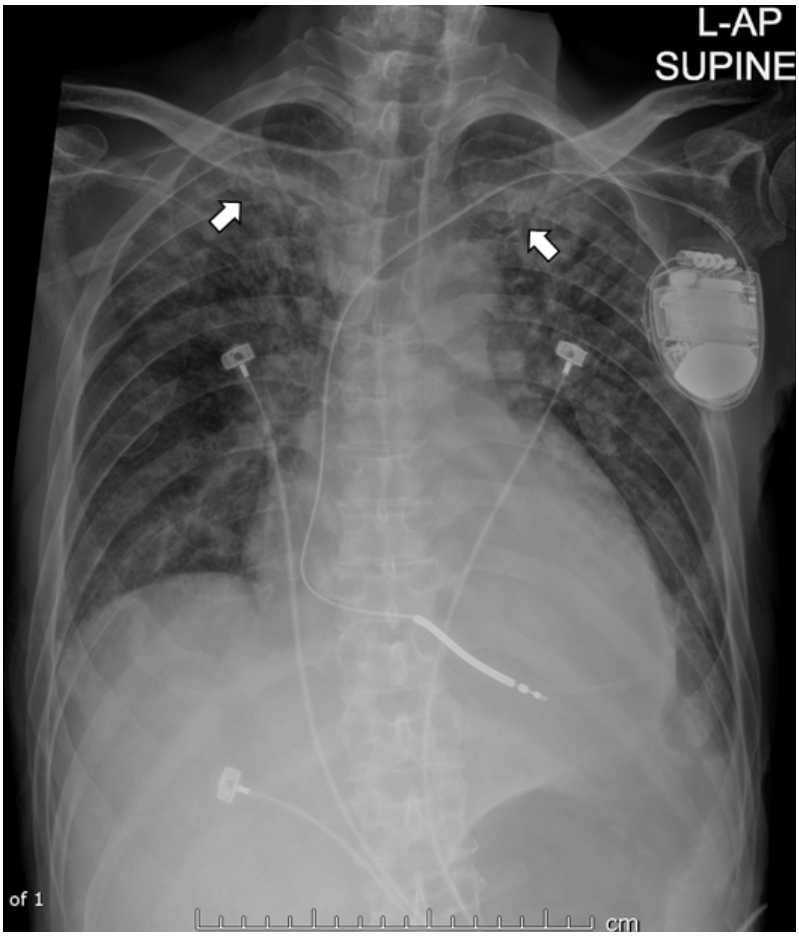

Figure 1. *AP supine portable chest radiograph reveals diffuse patchy opacification with air bronchogram (white arrows) in both lungs, predominantly in both upper lobes.*

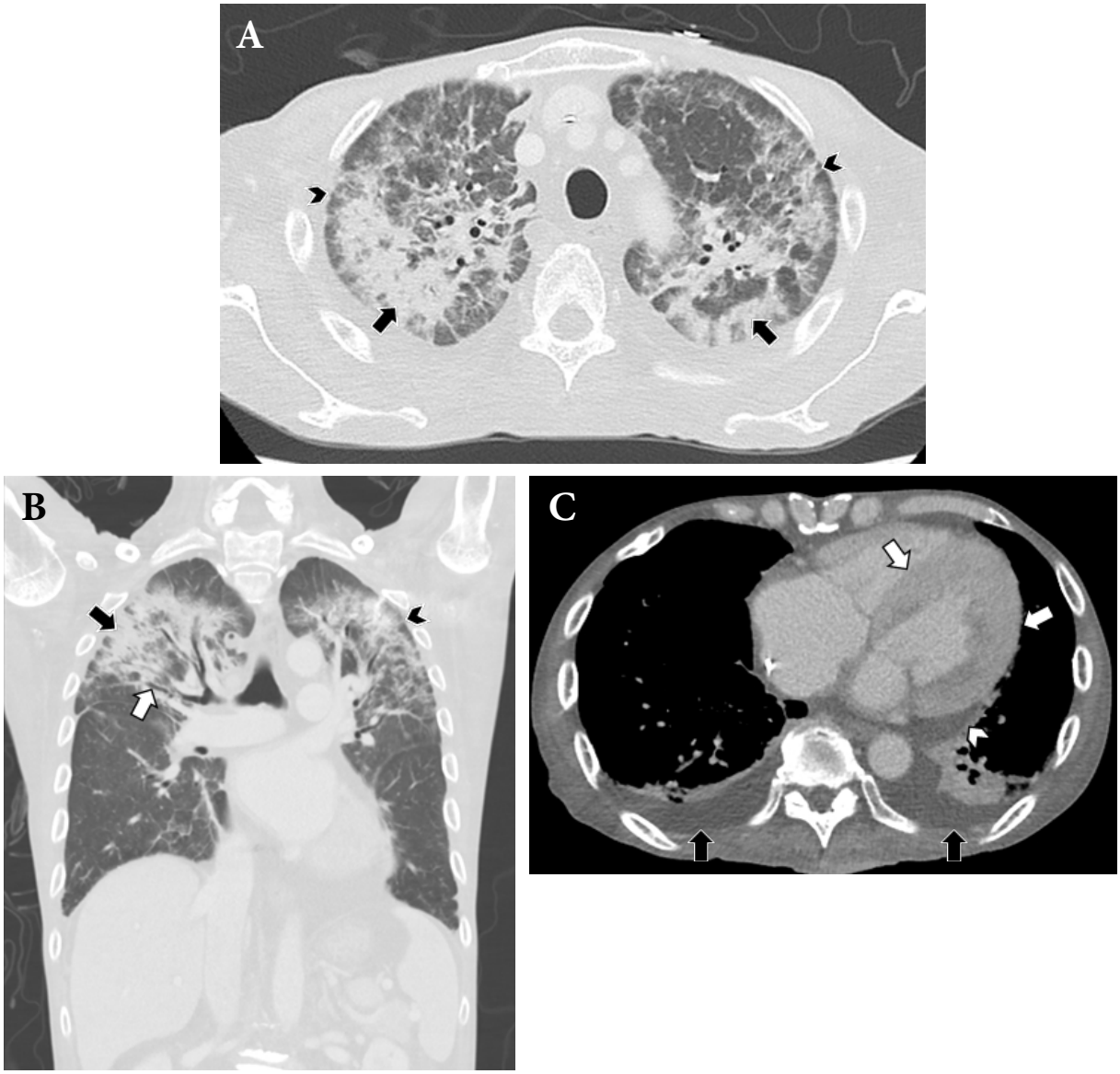

Figure 2. *Venous phase chest computed tomography (CT).*
(A, B) Lung window axial and coronal images show bilateral pulmonary consolidations (black arrows), ground-glass opacities with air bronchograms (white arrows), and interlobular septal thickening (black arrowheads) predominantly in both upper lobes.
(C) Mediastinal window axial image shows bilateral pleural effusions (black arrows), a common finding of pleural involvement of amyloidosis. Minimal pericardial effusion (white arrowhead), as well as concentric and symmetric left ventricular wall and interventricular septal thickening (white arrows) was also observed in this case, a common yet nonspecific finding in cardiac amyloidosis.

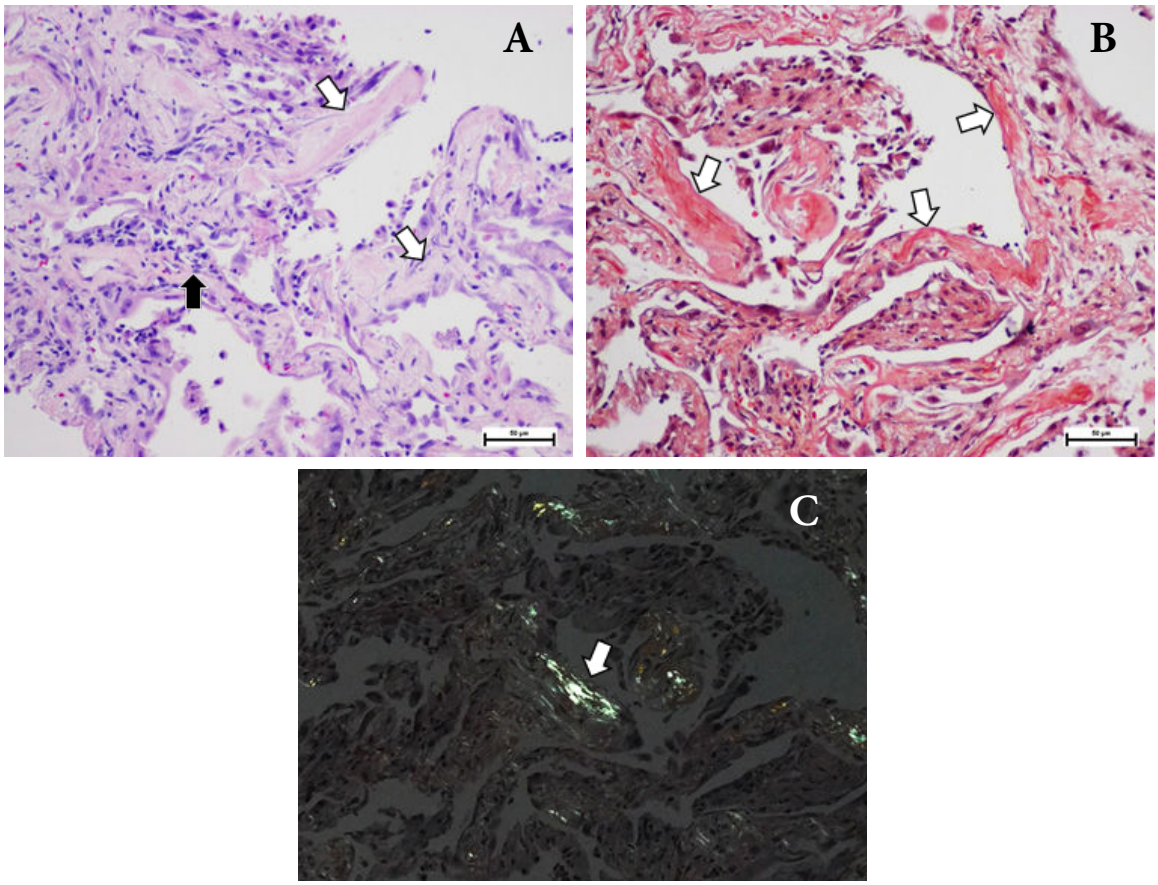

Figure 3. *Microscopic examination of the right upper lobe lung tissue biopsy.*
(A) The histology of the biopsied lesion shows benign alveoli with interstitial thickening with deposition of pink amorphous material (white arrows). The other area shows focal fibroblast proliferation with mild interstitial chronic inflammation (black arrows).
(B, C) Congo red staining shows the area of abnormal eosinophilic material in the interstitial area (B) and shows apple-green birefringence of the amyloid material in polarised light (C) (white arrows).

THE ASEAN JOURNAL OF RADIOLOGY
ISSN 2672-9393

Discussion

Pulmonary amyloidosis is a rare and lethal disease as it may cause pulmonary hypertension, respiratory failure, and eventually death. As described earlier, imaging findings of pulmonary amyloidosis are non-specific and the diagnosis of pulmonary amyloidosis still relies heavily on histopathological diagnosis. Previously reported imaging findings of nodular parenchymal amyloidosis includes solitary or multiple pulmonary nodules which may rarely calcify and cavitate, while diffuse alveolar septal amyloidosis may manifest as reticulonodular opacities, interlobar septal thickening, and confluent consolidations with basal and peripheral predominance in the lungs[1].

In the case of our patient, although his chest CT images revealed nonspecific findings as described, they do coincide with the previously reported findings of diffuse alveolar septal amyloidosis[1,6]. No nodules, calcifications, or cavitary lesions were detected in our case. The patient also had bilateral pleural effusions, which is the most common finding in pleural involvement of amyloidosis[1]. Although pulmonary amyloidosis usually involves basal and peripheral lungs, upper lung involvement of nodular parenchymal amyloidosis has been reported[7]. In addition, minimal pericardial effusion as well as concentric and symmetrical left ventricular wall and interventricular septal thickening was also observed in this case, a common yet nonspecific finding in cardiac amyloidosis[1,8].

In retrospect, taking into account the patient's underlying medical conditions of light chain multiple myeloma and systemic amyloidosis, one might consider that the patient may have pulmonary amyloidosis as well. However, due to the patient's clinical presentation mimicking that of pneumonia and pulmonary oedema, combined with nonspecific imaging findings which support both differential diagnoses, pulmonary amyloidosis was initially not suspected. The diagnosis of pulmonary amyloidosis in this patient was made through diagnostic bronchoscopy with histopathological evaluation from tissue biopsy alone. Our case further highlights the importance of maintaining a high clinical suspicion for

such a rare disease, especially in patients with underlying medical conditions with a high risk of pulmonary amyloidosis, and the importance of histopathological evaluation in cases of unresolving pneumonia.

Conclusion

We described a case of a 56-year-old male with a known history of multiple myeloma free light chain lambda with International Staging System (ISS) stage II, systemic amyloidosis and cardiac amyloidosis, diagnosed with biopsy-proven pulmonary amyloidosis manifesting as nonspecific imaging findings of the chest. The role of imaging studies in the diagnosis of pulmonary amyloidosis is still very limited due to nonspecific findings, but may help guide pneumologists in planning their bronchoscopy and location of tissue biopsy. The diagnosis in our case was made based on tissue biopsy with histopathological diagnosis alone which highlights the importance of maintaining a high clinical suspicion for such a rare disease, especially in patients with underlying medical conditions with a high risk of pulmonary amyloidosis, and the importance of histopathological evaluation in cases of unresolving pneumonia.

THE ASEAN JOURNAL OF RADIOLOGY
ISSN 2672-9393

References

1. Czeyda-Pommersheim F, Hwang M, Chen SS, Strollo D, Fuhrman C, Bhalla S. Amyloidosis: modern cross-sectional imaging. Radiographics 2015;35:1381–92. doi: 10.1148/rg.2015140179.

2. Baumann B, Salina D, Aboulhosn K. Clinical pulmonary amyloidosis presenting as lung cavitation with bronchiectasis: a case report. BCMJ 2019;61:344-8.

3. Blancas-Mejía LM, Ramirez-Alvarado M. Systemic amyloidoses. Annu Rev Biochem 2013;82:745–74. doi: 10.1146/annurev-biochem-072611-130030.

4. Li G, Han D, Wei S, Wang H, Chen L. Multiorgan involvement by amyloid light chain amyloidosis. J Int Med Res 2019;47:1778–86. doi: 10.1177/0300060518814337.

5. Lal A, Akhtar J, Khan MS, Chen Y, Yaron Goldman. Primary endobronchial amyloidosis: a rare case of endobronchial tumor. Respir Med Case Rep 2018;23:163–6. doi: 10.1016/j.rmcr.2018.02.007.

6. Georgiades CS, Neyman EG, Barish MA, Fishman EK. Amyloidosis: review and CT manifestations. Radiographics 2004;24:405–16. doi: 10.1148/rg.242035114.

7. Lee SH, Ko YC, Jeong JP, Park CW, Seo SH, Kim JT, et al. Single nodular pulmonary amyloidosis: case report. Tuberc Respir Dis (Seoul) 2015;78:385–9. doi: 10.4046/trd.2015.78.4.385.

8. Oda S, Kidoh M, Nagayama Y, Takashio S, Usuku H, Ueda M, et al. Trends in diagnostic imaging of cardiac amyloidosis: emerging knowledge and concepts. Radiographics 2020;40:961–81. doi: 10.1148/rg.2020190069.

ASEAN Movement in Radiology

Thailand's experience on radiation safety and quality practice in diagnostic radiology

Napapong Pongnapang, Ph.D.
From Department of Radiological Technology, Faculty of Medical Technology, Mahidol University, Bangkok, Thailand.
Address correspondence to N.P. (e-mail: napapong.pon@mahidol.ac.th)

Received 24 December 2020; accepted 25 December 2020
doi:10.46475/aseanjr.v21i3.101

Keywords: Thailand, Radiology, Radiation safety, Quality.

Radiology services in Thailand started in 1898 by Professor Hans Adamsen, a royal court physician, who brought the first x-ray machine to the country. Thailand's radiology education and training started in 1928 by Professor Pin Muangman, a pioneer radiologist who graduated from Harvard University, USA. At present, Thailand has 1950 radiologists, 200 medical physicists and 5200 radiological technologists practicing in the healthcare system. Radiology services in Thailand started in 1898 by Professor Hans Adamsen, a royal court physician, who brought first x-ray machine to the country. Thailand Radiology education and training started in 1928 by Professor Pin Muangman (Figure 1), a pioneer radiologist who graduated from Harvard University, USA. At present, Thailand has 1950 radiologists, 200 medical physicists and 5200 radiological technologists practicing in the healthcare system.

THE ASEAN JOURNAL OF RADIOLOGY
ISSN 2672-9393

Figure 1. *Professor Pin Muangman, M.D., founder of Thailand's Radiology.*

A main radiation safety control is under the Nuclear Power Safety Act (updated in 2016). Radiologists and Technologists' professional practices are controlled under a relevant professional law while the medical physicists licensing will be effective by 2021. An updated regulation stipulates that all radiation emitting machines (in diagnostic radiology and dentistry) are required to be registered at the Ministry of Public Health. Annual safety and quality investigation of x-rays equipment is required to be performed by the physicists.

As a UN member state, Thailand has been actively participating in a number of projects related to quality and safety in diagnostic radiology with the International Atomic Energy Agency (IAEA). Following corresponding requests, usually linked, but not limited to relevant TC projects, the IAEA is responsible for forming the auditing team, giving an international perspective and assuring the principle of independency between the auditors and the audited department. The IAEA clinical audit program (QUAADRIL) was extablished in Thailand in 2017 (Figure 2) with a future plan to adopt the system and transfer it to Thai-QUAADRIL.

Figure 2. *IAEA Expert mission to train local professions on radiation safety and quality practice in diagnostic radiology.*

Regarding optimization of medical exposure, setting up the Diagnostic Reference Levels (DRLs) is a tool for optimizing radiation dose which further leads to a safe use of diagnostic radiation. The DRLs project has been carried out by Thailand Ministry of Public Health since 2017 (Figure 3). Currently, DRLs values plain and dental radiography, computed tomography and mammography. The plan is now extended to include Interventional Radiology. National Dose Index Registry starts in the US under the American College of Radiology (ACR). The first high dose modality to be registered is Computed Tomography (CT). Thailand under the IAEA project received the permission to start the first phase of the DIR in 2020. The main purposes of the DIR are to optimize the patient dose and to set up national DRLs on the modality.

Figure 3. *Training on data collection and establishment of the Diagnostic Reference Levels (DRLs) for physicists from the Ministry of Public Health.*

In summary, quality and safety in diagnostic radiological services are key elements utilized by the practicioners to ensure the best benefits to patients. We have a future plan to establish Thailand's clinical audit system for radiological services with collaboration among professional bodies (radiologists, medical physicists and radiological technologists). The Diagnostic Reference Levels (DRLs) will be updated every 5 years. The patient dose audit system will also be established. Our experience showed that multi-professional collaboration is a key for success in patient safety and quality in diagnostic radiology.

ASEAN

This journal provide 4 areas of editorial services: language editing, statistical editing, content editing, and complete reference-citation check in 8 steps:

Step	Services to authors	Services providers
I	Manuscript submitted	Editor
II	Language editing/ A reference-citation check	Language consultant/Bibliographer
III	First revision to ensure that all information remains correct after language editing	Editor
IV	Statistical editing	Statistical consultant
V	Content editing*	Two reviewers
VI	Second revision	Editor
VII	Manuscript accepted/ rejected	Editor/Editorial board
VIII	Manuscript published	Editorial office

*Content editing follows a double-blind reviewing procedure

JOURNAL OF RADIOLOGY